

## HETGS Update

### Herman Marshall

The High Energy Transmission Grating Spectrometer [HETGS, 1] is essentially unchanged since launch. The grating efficiencies were updated in 2011 to bring the high and medium energy grating spectra into better agreement (see the HETGS article in Issue 19 of the *Chandra* Newsletter). Here, I present an update of two possible calibration issues and a summary of some interesting new HETGS results.

For the recent *Chandra* Users Committee (CUC) meeting,<sup>1</sup> I was asked to present two topics. The first one relates to a report that the HETGS line response function (LRF) may require adjustment. The second is about our on-going effort to cross-calibrate the HETGS with other instruments such as *XMM-Newton* and *NuSTAR*.

#### Line Response Function

Liu (2016, [2]) examined the Fe K $\alpha$  lines of several active galactic nuclei (AGN) to examine their emission line regions. Liu examined the second and third order versions of the line to improve spectral resolution, which is highly recommended to all HETGS observers when there is sufficient signal. However, the energy dispersions  $\sigma_E$  derived from orders  $\pm 2$  and  $\pm 3$  were found to be smaller than that of order  $\pm 1$  for all AGN in the sample. I examine this discrepancy in this article.

The sample used by Liu consisted of nearby, bright Seyfert galaxies. These include the Circinus galaxy, NGC 4151, NGC 3783, Mrk 3, and NGC 1068. The discrepancies between first order and high orders was most significant for two galaxies, Circinus and Mrk 3, where  $\sigma_E = 6.2 \pm 1.4$  eV and  $4.9^{+5.2}_{-4.9}$  eV for first order but  $9.8 \pm 0.9$  eV and  $19.0 \pm 3.9$  eV for the combination of second and third orders, respectively. While the individual significances are less than  $3\sigma$ , collectively, the sample showed smaller energy dispersions for high orders than for first order. Liu suggested that line widths measured were “over-estimated” in first order spectra.

Besides being bright, these Seyfert galaxies share another characteristic: they all have X-ray emission extended on a scale of 3-10" as clearly imaged with *Chandra*. Figure 1 shows that the gratings were generally oriented so that the dispersion axis was along the dimension of smallest extent, extent still plays an important role when measuring emission lines.

Quantitatively, one may model a Gaussian line with several contributions to assess the effect of spatial broadening on linewidth. Suppose that all effects have profiles given by Gaussians, with the instrumental broadening given by  $\sigma_i$  in detector space, Doppler broadening given by  $\sigma_v$  in velocity space, and spatial broadening given by  $\sigma_\theta$  in imaging space. Converting each to their effect on the total broadening in

physical coordinates  $x$  on the detector for wavelength  $\lambda$  and remembering the grating equation  $m\lambda = P \sin \alpha = Px/R$  (for small dispersion angles) gives

$$\sigma_x^2 = \sigma_i^2 + (Rm\lambda/Pc)^2 \sigma_v^2 + (F\sigma_\theta)^2 \quad (1)$$

where  $m$  is the grating order,  $P$  is the grating period,  $R$  is the Rowland distance of the HETGS, and  $F$  is the focal length of the HRMA.

Eq. 1 shows that imaging is more important than instrumental broadening when  $F\sigma_\theta \gg \sigma_i$ ; i.e., when a source is resolved. More importantly, instrumental and imaging terms dominate when  $m\sigma_v$  is small but as  $m$  increases, the linewidth is dominated Doppler broadening. Thus, spatial extent can be ignored only if  $\sigma_v \gg 3400 \sigma_\theta/m\lambda$  km/s for  $\lambda$  in  $\text{\AA}$  and  $\sigma_\theta$  in arcsec. For a resolvable source with  $\sigma_\theta = 1''$  and examining the Fe K $\alpha$  line at  $1.94 \text{ \AA}$  using the high energy gratings, then spatial extent is comparable to Doppler broadening when  $\sigma_v = 1750$  km/s. In third order, however, this cross-over value drops to 600 km/s. Hence it is clearly advantageous to examine the high order HETGS data where feasible. Figure 2 illustrates this point from profiles of the Fe K $\alpha$  line as observed from the Circinus galaxy. The 0<sup>th</sup> order profile was fit by a Gaussian, whose dispersion is only about 30% larger than expected for a point source. The dispersed spectra are progressively wider with grating order, as expected when Doppler broadening is increasingly important relative to spatial and instrumental broadening.

Figure 3 shows HETGS spectra of unresolved stars without significant Doppler motions due to companions [3]. The Fe xxv line at  $1.85 \text{ \AA}$  is unresolved with limits to Doppler broadening at about 100 km/s. These data probably provide the best test of the HETGS LRF and indicate that the released response matrices are adequate for AGN spectroscopy.

#### Cross Calibration of X-ray Telescopes

The *Chandra* Calibration team has been working on cross-calibration of instruments since launch. In 2005, we teamed up with the *XMM-Newton* calibration scientists to initiate the International Astronomical Consortium for High Energy Calibration (IACHEC) and held our first meeting in 2006. Every high energy mission is or has been represented at our annual meetings. Presentations for all meetings and results from working groups are public.<sup>2</sup>

Recent results from the work of IACHEC include papers on cross-calibration between *NuSTAR*, *Swift*, *Chandra*, *XMM-Newton*, and *Suzaku* using simultaneous observations of two blazars: 3C 273 and PKS 2155-304. Results were published earlier this year by Madsen et al. [4]. Madsen et al. cross-checked instruments pairwise, to ensure significant exposure overlap, measuring fluxes in the 1-5 keV or 3-7 keV bands. There were several disagreements at the 5-10% level, where the HETGS gives higher fluxes than most other missions. These results are similar to those of a

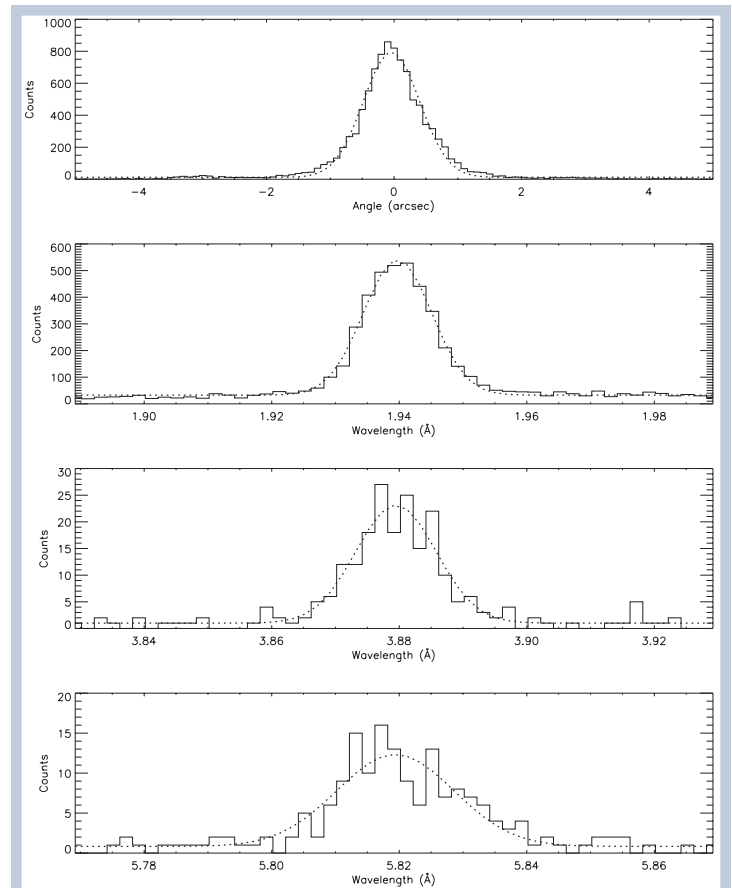
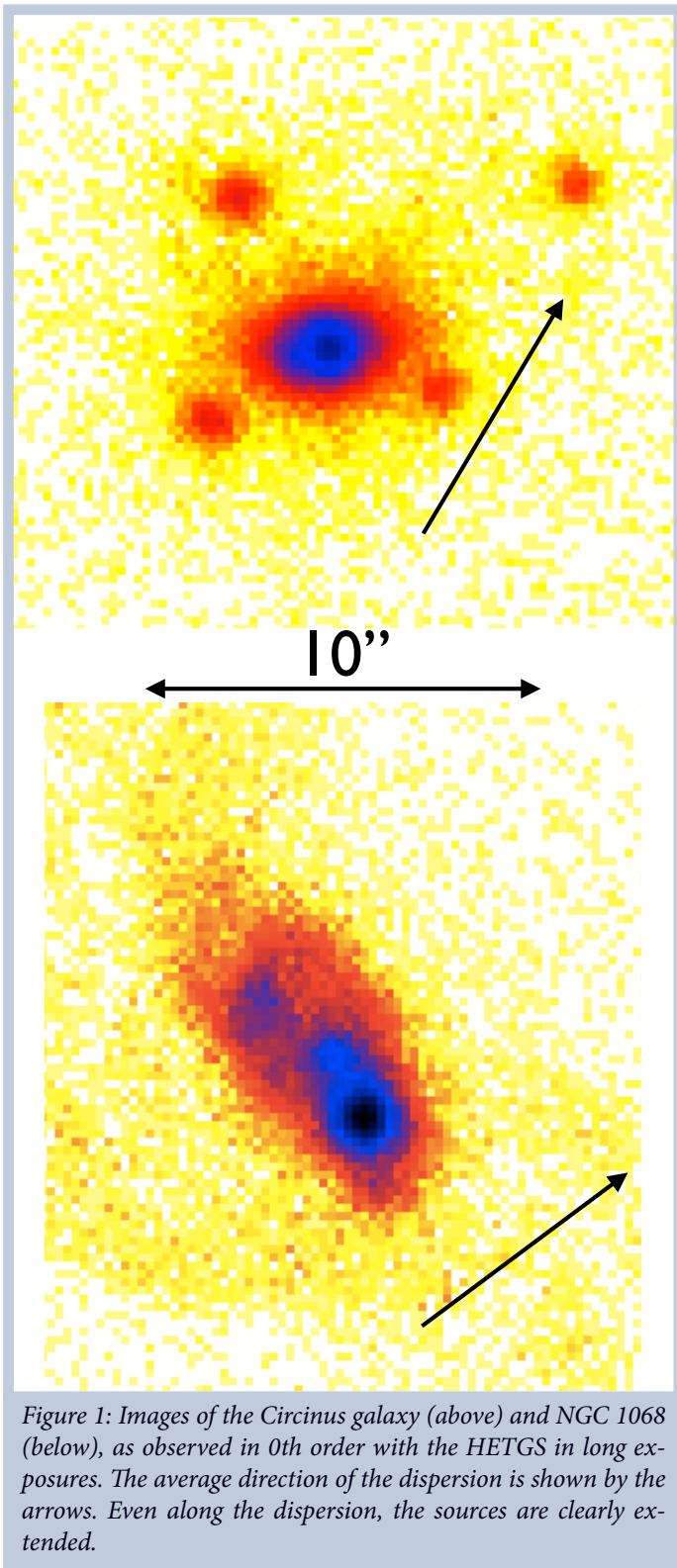


Figure 2: Average profiles taken from many HETGS observations of the Circinus galaxy. Top: Profile of zeroth order (5-6 keV) projected onto the dispersion line of the high energy gratings and fit to a Gaussian. The dispersion of the Gaussian is 0.44", about 30% larger than expected for a point source. 2nd from top: Profile of the Fe K $\alpha$  line in  $\pm 1$  orders, summed and fit to a Gaussian. The wavelength region plotted matches the projected angular range of zeroth order and the profile is marginally wider than that of zeroth order due to Doppler broadening. 2nd from bottom: Profile of the Fe K $\alpha$  line in  $\pm 2$  orders, as in the panel above. Note that the line appears somewhat broader than in first order. Bottom: Profile of the Fe K $\alpha$  line in  $\pm 3$  orders, as in the panel above. Note that the line appears significantly broader than in first order. The extra width is due to Doppler broadening.

previous IACHEC paper by Ishida et al. (2011, [5]) but with a lower level of significance. In a comparison to RXTE, Guver et al. (2016, [6]) found agreement between HETGS and RXTE in the 2-8 keV range to better than 2% using X-ray bursts from GS 1826-238.

By contrast in method, Plucinsky et al. (2017, [7]) used emission lines of highly ionized atoms of O and Ne in the 0.5–1.0 keV range from the supernova remnant 1E 0102.2-7219 to compare the same missions (excluding *NuSTAR*). In this case, the HETGS agrees within 5-10% of the (somewhat arbitrary) reference fluxes. There is significant scatter between instruments, with some high by 10% across the board and some low by 10%.

All these efforts to compare instruments provide the raw data needed to assess systematic errors in instrument calibration. The studies did not aim to actually suggest or encourage corrections but to help users bound potential systematic errors. Generally, we conclude from IACHEC studies that fluxes derived from most X-ray instruments agree to 10% but there are cases where the disagreement between two telescopes is 20% or more, depending on the

energy of interest. There are two questions that naturally arise from these findings: “What can we do to obtain agreement?” and “Which instrument is right?” Absolute calibration is extremely difficult, as one might imagine based on decades of work to establish optical photometric standards. So, for now, we set aside the second question and try to answer the first one.

Meanwhile, there are several efforts within IACHEC to devise a way to bring the results from X-ray telescopes into better agreement.<sup>3</sup> One of these is called the “Concordance” project. Outlined at the 2015 meeting of the IACHEC, the goal is to develop a statistical formalism that uses estimates of a priori systematic errors, based on ground calibration and internal flight calibration data. The statistical method is based on “shrinkage estimators”, which use the population of results to infer biases (systematic errors) in the outlying measurements. The project is a collaboration between X-ray calibration scientists in the *Chandra* calibration group—Jeremy Drake, Vinay Kashyap, and me—and members of the Harvard University Statistics Department: Prof. Xiao-Li Meng and two students, Yang Chen and Xufei Wang. Chen

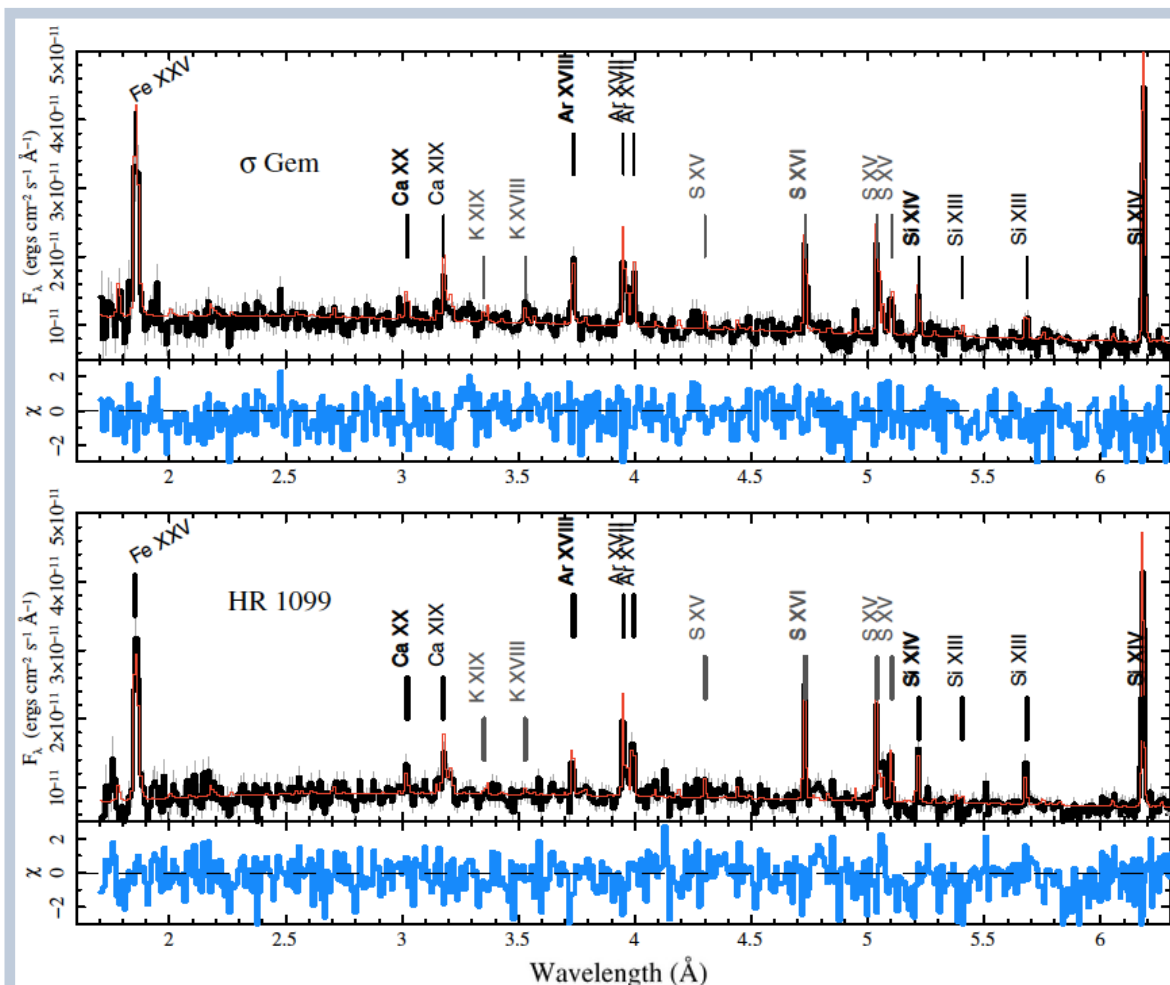


Figure 3: HETGS spectra of two stars [3]. The Fe xxv lines of both are consistent with the expected instrumental resolution.

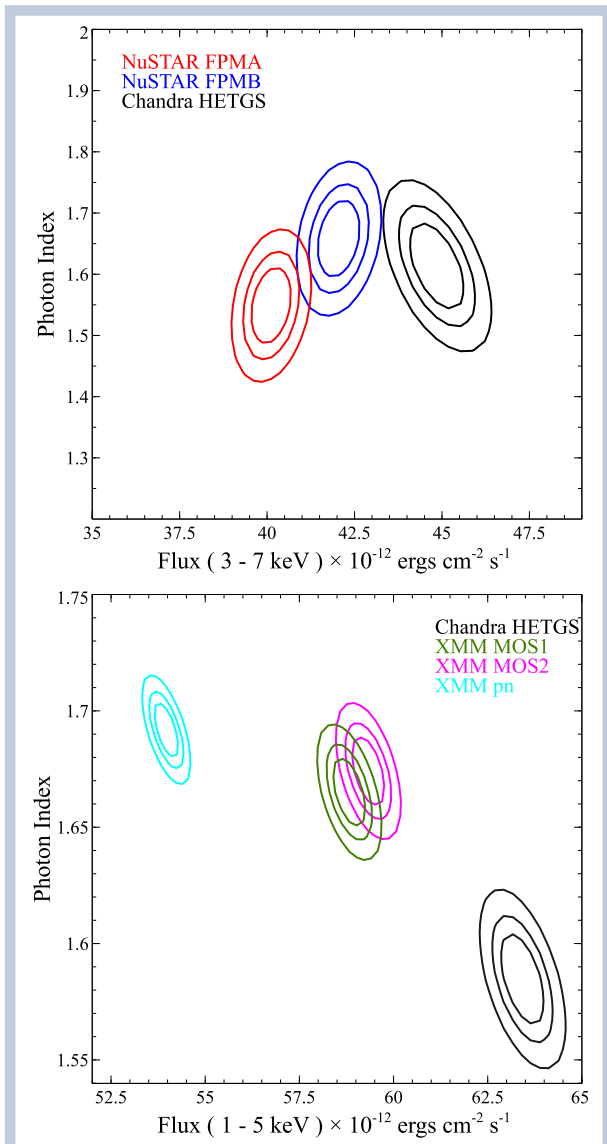


Figure 4: Two figures from Madsen et al. (2017, [4]) cross-checking fluxes determined from HETGS observations taken simultaneously with NuSTAR (top) or XMM-Newton (bottom). These cross-calibration campaigns serve to provide data that will be used to improve spectral agreement between missions.

will lead a paper on the methodology for a statistics journal and I will lead one for an astrophysics journal. See presentations to the CUC and IACHEC for details.

Other IACHEC work focuses on how to analyze data when systematic errors are characterized. These include py-BLoCXS [8, 9] and MCCal [10], all involving *Chandra* calibration scientists. These studies have been used to demonstrate the limitations to measuring spectral parameters in the presence of systematic errors. Drake et al. (2006, [10]), for example, found that systematic errors can dominate the uncertainties in a spectral parameter such as the power law spectral index or thermal temperature when an ACIS observation has as few as  $10^4$  counts. Again, there are IA-

CHEC presentations about these methods that can provide more details.

### Recent HETGS Highlights

The High Energy Transmission Grating Spectrometer continues to provide excellent spectra for detailed examination of source properties. In particular, two papers show very nice spectra of X-ray binaries at high resolution. Miškovičová et al. (2016, [11]) found P Cygni profiles in the HETGS spectrum of Cyg X-1. Figure 5 shows P Cygni profiles in many emission lines, informing a model of the focused wind from the companion. They measure wind velocities, column densities, and gas temperatures. From the Mg xi triplet near  $9.2 \text{ \AA}$  can be derived a density estimate of up to  $4 \times 10^{13} \text{ cm}^{-3}$  in the wind.

Miller et al. (2016, [12]) obtained the HETGS spectrum of GX 340+0 in a state that shows strong absorption at 6.9 keV (see Figure 6). If interpreted as absorption by Fe xxv, then the wind velocity is  $0.04c$ . They suggest that the wind is driven by radiation pressure, in a manner analogous to broad absorption features in some quasars because the gas has some low ionization components. Depending on the filling factor of the wind, the kinetic power of the outflow may exceed the luminous power of the disk around the neutron star in the X-ray binary. ■

### Footnotes

- 1 The meeting was held on 27 September 2016. See [http://asc.harvard.edu/cdo/cuc/cuc\\_file16/sep27/](http://asc.harvard.edu/cdo/cuc/cuc_file16/sep27/) for the agenda and presentations.
- 2 See the IACHEC web site <http://web.mit.edu/iachec/> for more details.
- 3 For an overview of the efforts of the IACHEC Calibration Uncertainty Working Group, see the IACHEC 2016 summary by Vinay Kashyap, which includes references to other presentations.

### References

- [1] Canizares, C.R., et al., 2005, PASP, 117, 1144.
- [2] Liu, J. 2016, MNRAS, 463, L108
- [3] Huenemoerder, D.P., et al., 2013, ApJ, 768, 135.
- [4] Madsen, K. K., Beardmore, A. P., Forster, K., et al. 2017, AJ, 153, 2
- [5] Ishida, M., Tsujimoto, M., Kohmura, T., et al. 2011, PASJ, 63, S657
- [6] Güver, T., Ö, F., Marshall, H., et al. 2016, ApJ, 829, 48
- [7] Plucinsky, P. P., Beardmore, A. P., Foster, A., et al. 2017, A&A, 597, A35
- [8] Xu, J., van Dyk, D. A., Kashyap, V. L., et al. 2014, ApJ, 794, 97
- [9] Lee, H., Kashyap, V. L., van Dyk, D. A., et al. 2011, ApJ, 731, 126
- [10] Drake, J. J., Ratzlaff, P., Kashyap, V., et al. 2006, Proceedings SPIE, 6270, 62701I
- [11] Miškovičová, I., Hell, N., Hanke, M., et al. 2016, A&A, 590, A114
- [12] Miller, J. M., Raymond, J., Cackett, E., Grinberg, V., & Nowak, M. 2016, ApJ, 822, L18

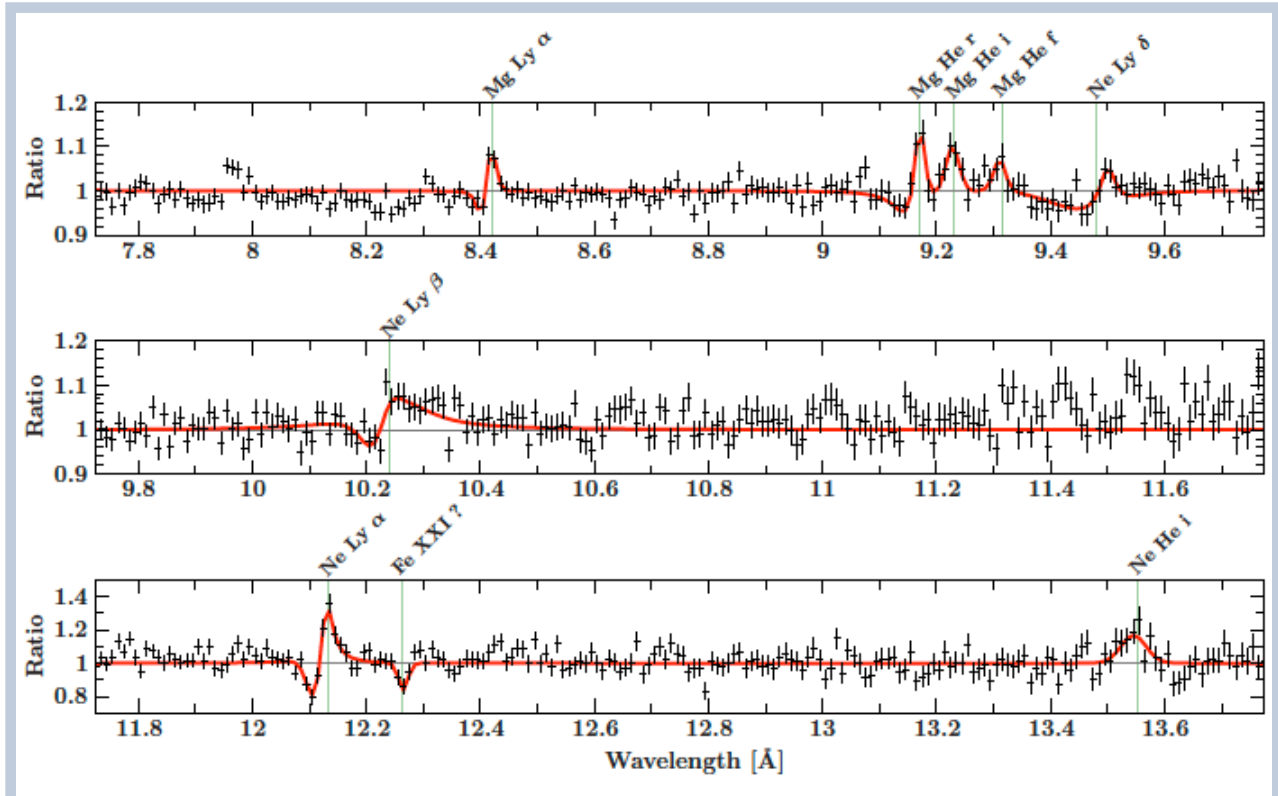


Figure 5: A portion of the HETGS spectrum of Cyg X-1 from ObsID 11044 (Miškovičová et al (2016, [11])). The data were divided by a model consisting of a power law absorbed by cold gas. Several lines show P Cygni profiles, such as Mg Ly $\alpha$ , Ne Ly $\alpha$ , and even Ne Ly $\beta$ . The observation is from inferior conjunction, where the disk wind is observed most clearly. Components of He-like Mg XI are readily discerned, providing density diagnostics.

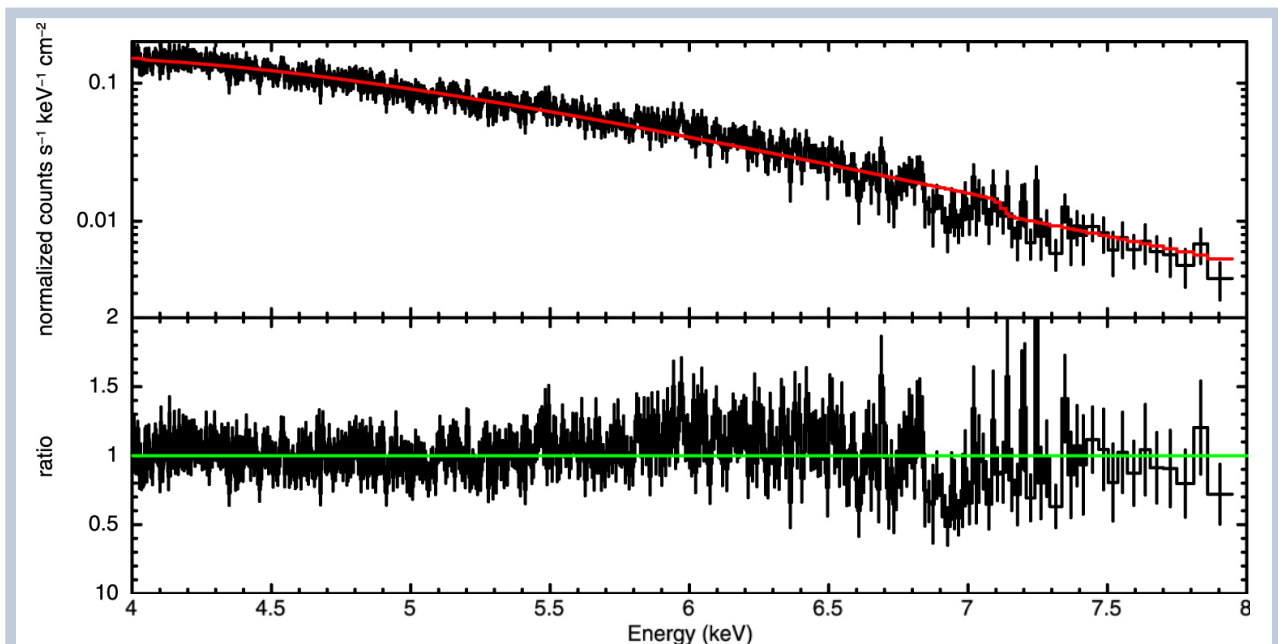


Figure 6: The 4-8 keV spectrum of GX 340+0 from Miller et al. (2016, [12]), ObsID 1922. The fit is to a disk blackbody (top panel) and the ratio to the model is given in the lower panel. The absorption feature near 6.9 keV was modeled as due to Fe XXV with an outflow velocity of  $0.04c$ .